GDCh

Communications

Angewandte
Chemie
International Edition
www.angewandte.org

Solid-State Chemistry

Structural Influence of Lone Pairs in GeP$_2$N$_4$, a Germanium(II) Nitridophosphate

Sebastian J. Ambach, Cody Somers, Tristan de Boer, Lucien Eisenburger, Alexander Moewes, and Wolfgang Schnick*

Abstract: Owing to their widespread properties, nitridophosphates are of high interest in current research. Explorative high-pressure high-temperature investigations yielded various compounds with stoichiometry MP_2N_4 ($M=$Be, Ca, Sr, Ba, Mn, Cd), which are discussed as ultra-hard or luminescent materials, when doped with Eu^{2+}. Herein, we report the first germanium nitridophosphate, GeP$_2$N$_4$, synthesized from Ge$_3$N$_4$ and P$_3$N$_5$ at 6 GPa and 800 °C. The structure was determined by single-crystal X-ray diffraction and further characterized by energy-dispersive X-ray spectroscopy, density functional theory calculations, IR and NMR spectroscopy. The highly condensed network of PN$_4$-tetrahedra shows a strong structural divergence to other MP_2N_4 compounds, which is attributed to the stereochemical influence of the lone pair of Ge^{2+}. Thus, the formal exchange of alkaline earth cations with Ge^{2+} may open access to various compounds with literature-known stoichiometry, however, new structures and properties.

$\boldsymbol{N}$itridophosphates are an extremely diverse class of materials attracting high interest in current research. Their wide range of applications and intriguing materials properties emerge from the structural versatility, which competes with the earth's predominant class of materials, the (oxo)silicates.[1] Due to the isoelectronic combination of elements Si/O and P/N, both form similar structural motifs, most commonly SiO$_4$- and PN$_4$-tetrahedra. In the majority of cases, these building blocks are arranged in three-dimensional anionic networks or two-dimensional layers. The isoelectronic relation is mirrored in analogous crystal structures of oxosilicates and nitridophosphates, e.g. the

silicate mineral paracelsian BaAl$_2$Si$_2$O$_8$ and LiNdP$_4$N$_8$ or the recently discovered mica analogues AESi$_3$P$_4$N$_{10}$(NH)$_2$ ($AE=$ Mg, Ca, Sr) as well as various SiO$_2$ analogue modifications of PON.[2–8] Due to the fact that N can connect up to three tetrahedra in nitridophosphates and features both corner and edge sharing connections, while O in oxosilicates usually is limited to two connections and corner sharing, the structural versatility of the former may even surpass the one of the latter. Consequently, the degree of condensation κ, given as the atomic ratio between tetrahedral centres (T) and ligands (X) by $\kappa={}^{N(T)}\!/_{N(X)}$, is limited to a maximum of $^1\!/_2$ in oxosilicates (SiO$_2$), but can reach a maximum of $^3\!/_5$ in nitridophosphates (P$_3$N$_5$).[9]

Even though most highly condensed ($\kappa\geq{}^1\!/_2$) nitridophosphates are stable under ambient conditions, their initial synthesis remains a sophisticated issue. In presence of oxygen, the formation of oxides is favored over the formation of nitrides, as P–O-bonds are more stable than P–N-bonds. Furthermore, owing to the positive electron affinity of N, nitride ions are prone to oxidation and the formation of N$_2$ at elevated temperatures, while P^V may easily be reduced to P^{III} or P^0 or even P^{-III}. P$_3$N$_5$, a key precursor in many nitridophosphate syntheses, for instance, decomposes at 850 °C, while usually temperatures above 1000 °C are necessary for product crystallization.[10] Following Le Chatelier's principle, decomposition can be suppressed by applying pressure, which enables high temperature syntheses.

Employing the high-pressure approach, explorative research yielded numerous highly condensed nitridophosphates. Compounds with a degree of condensation of $\kappa=^1\!/_2$, for example, were found for a broad variety of cations and show intriguing materials properties. In the group of APN$_2$ ($A=$H, Li, Na), LiPN$_2$ was discussed for its Li-conductivity, while HPN$_2$ is a sought-after precursor for nitridophosphate synthesis.[11–15] AEP$_2$N$_4$ ($AE=$Be, Ca, Sr, Ba) shows exceptional high hardness for Be in case of a high-pressure modification as well as promising luminescent properties in case of Ca, Sr and Ba, when doped with Eu^{2+}.[16–19] Furthermore, it was even possible to synthesize two of the first transition metal nitridophosphates, namely MP_2N_4 ($M=$ Mn, Cd).[20] Most synthetic approaches for these compounds start from metal azides in combination with HPN$_2$ or P$_3$N$_5$. Due to their explosiveness, the azides may be replaced by the respective metal nitrides or even metal powders. Most named compounds incorporating a cation with charge +2 (Ca^{2+}, Sr^{2+}, Mn^{2+}, Cd^{2+}) crystallize isotypically in a structure closely related to the megacalsilite (KAlSiO$_4$) type.[21]
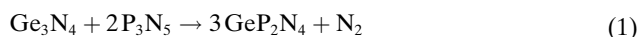
[*] M. Sc. S. J. Ambach, Dr. L. Eisenburger, Prof. Dr. W. Schnick
Department of Chemistry, Ludwig-Maximilians-University Munich
Butenandtstraße 5–13, 81377 Munich (Germany)
E-mail: wolfgang.schnick@uni-muenchen.de

C. Somers, Dr. T. de Boer, Prof. Dr. A. Moewes
Department of Physics and Engineering Physics, University of Saskatchewan
116 Science Place, Saskatoon, Saskatchewan, S7 N 5E2 (Canada)

BeP_2N_4 and BaP_2N_4 exhibit their own structure types, however, with related structural units.

In this contribution, we present GeP_2N_4, the first representative of germanium(II) nitridophosphates and the first compound in this class with a degree of condensation of $\frac{1}{2}$ incorporating a p-block cation. The title compound was synthesized under high-pressure high-temperature conditions at 6 GPa and 800 °C in a 1000 t hydraulic press with a modified Walker-type module. According to equation (1) GeP_2N_4 is formed from Ge_3N_4 and P_3N_5 by reduction of Ge^{IV} to Ge^{II} and partial oxidation of N^{-III} to N^0 in N_2. A second synthetic approach starts from elemental Ge, P_3N_5 and NH_4N_3 (equation 2).

$$Ge_3N_4 + 2P_3N_5 \rightarrow 3GeP_2N_4 + N_2 \tag{1}$$

$$3Ge + 2P_3N_5 + NH_4N_3 \rightarrow 3GeP_2N_4 + 2H_2 + N_2 \tag{2}$$

The starting materials were finely ground under argon atmosphere, tightly packed into an h-BN crucible and reacted in the multianvil apparatus, yielding a dark gray powder.[22] Further details on the synthesis are given in the Supporting Information. A reaction temperature of exactly 800 °C is necessary, as temperatures below 800 °C lead to an incomplete reaction, whilst temperatures above 800 °C already degrade GeP_2N_4 to elemental Ge and an amorphous side phase, most likely containing the remaining P and N. This temperature dependence was already observed for nitridogermanates, e.g. $Ca_{1-x}Li_xAl_{1-x}Ge_{1+x}N_3$ ($x \approx 0.2$).[23] Even at 800 °C, GeP_2N_4 starts to decompose in small amounts during synthesis. Decomposition products, especially elemental Ge, however, can be removed by washing the sample with a 1:1 vol-% mixture of 30 % H_2O_2 and concentrated NaOH. The washed samples contain single crystals up to 20 μm length, as shown by scanning electron microscopy (SEM) images (figures 1 and S1). The elemental composition of GeP_2N_4 was analyzed and confirmed by energy dispersive X-ray spectroscopy (EDX) measurements (table S1).

The structure of GeP_2N_4 was elucidated from inversion twinned single-crystal X-ray diffraction data ($Pna2_1$ (no. 33), $a = 9.547(1)$, $b = 7.542(1)$, $c = 4.6941(6)$ Å, $Z = 4$, $R_1 = 0.0240$; more details can be found in the Supporting Information).[24] The polar space group $Pna2_1$ allows potentially intriguing materials properties, such as pyro-, piezo- or ferroelectricity,
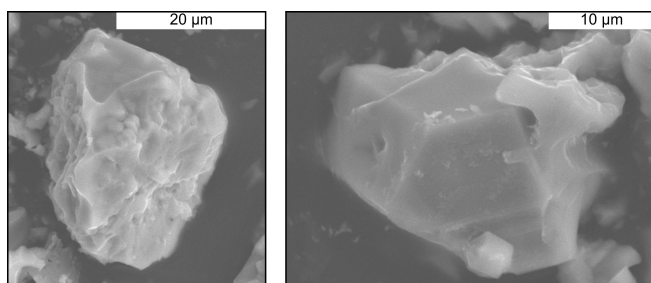
an electrooptic effect or second harmonic generation. Using the structure model combined with powder X-ray diffraction data, GeP_2N_4 was identified as the main constituent of samples by Rietveld refinement (figure S3).

In contrast to most MP_2N_4 phases, which crystallize isostructurally ($M = $ Ca, Sr, Mn, Cd) or consist of similar structural units ($M = $ Be), the structure of GeP_2N_4 shows only few similarities to the aforementioned. It is built up from all-side vertex-sharing PN_4-tetrahedra, forming a three-dimensional anionic P/N-network. The network can be described by undulated chains of PN_4-tetrahedra (blue, orange) along [100], which consist of pairs of two tetrahedra, pointing alternately up and down along [010] (figure 2). The connection of these chains form stacked *vierer* and *achter* rings along [001] as defined by Liebau.[1]

Two Ge^{2+}-ions are located within each *achter* ring, while the *vierer* rings stay empty. The point symbol, describing the network topology, was determined by the TOPOS software to be $\{4^2.6^3.8\}$, which matches with the paracelsian and $LiNdP_4N_8$ framework.[2,3,25] Whilst the anionic P/N framework is similar to the one of paracelsian and $LiNdP_4N_8$, the cation positions are not. Viewing along [001], Ba in paracelsian and Nd in $LiNdP_4N_8$ are located along the longitudinal axis of the *achter* rings, whereas Ge is located on the shorter transverse axis (figure S2). We attribute this structural divergence to a strong stereochemical effect of the lone pair at Ge^{2+}, forcing the cations onto positions with the least electrostatic repulsion. We assume that for the same reason the crystal structure of GeP_2N_4 shows no relation to other MP_2N_4 ($M = $ Be, Ca, Sr, Ba, Mn, Cd) phases, with the exception of PN_4-tetrahedra as basic building blocks. This feature is unprecedented in nitridophosphates, however, was theoretically investigated by Dronskowski et al. for alkaline-earth transition-metal chalcogenides.[26]

Distances (1.596(3)–1.654(4) Å) and angles (102.42(19)–117.4(2)°) in PN_4-tetrahedra of GeP_2N_4 are comparable to $LiNdP_4N_8$ and other MP_2N_4 ($M = $ Be, Ca, Sr, Ba, Mn, Cd) compounds. Ge^{2+} is threefold coordinated by N, forming a

Figure 1. Exemplary SEM images of single crystals of GeP_2N_4. Crystals are up to 20 μm in length and width.
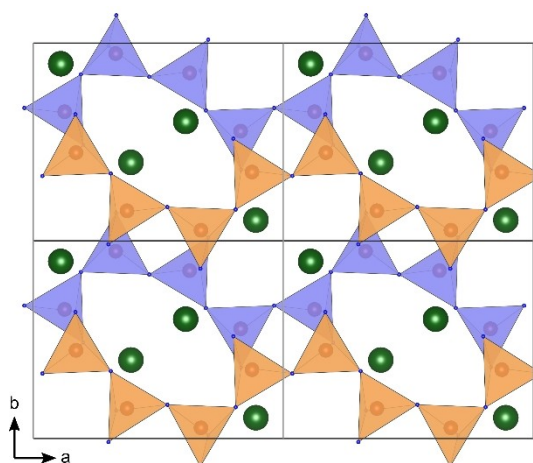

Figure 2. The crystal structure of GeP_2N_4 consists of all-side vertex-sharing PN_4-tetrahedra, forming undulated chains along [100] (orange, blue). The chains are interconnected and form *vierer* and *achter* rings.

trigonal pyramid (figure 3). Thus far, this coordination geometry is unprecedented in solid-state materials, which tend to form angled GeN_2^{4-}-units, e.g. in $Ba_3Ge_2N_2$, and was only observed in molecules, e.g. various aza-macrocyclic complexes.[27,28] DFT calculations support the observed bonding situation of Ge. Visualizing the electron density, it shows electron density between Ge1 and all coordinating nitrogen atoms N1/N2/N4 (figure 4). All three interatomic Ge–N distances (2.012(5)–2.150(4) Å) and N–Ge–N angles (85.87(15)–92.78(15)°) are in a close range and thus support the bonding situation, too. The Ge–N distances in GeP_2N_4 are slightly longer compared to those of the angled GeN_2^{4-}-units in $Ba_3Ge_2N_2$ (1.873(8)–1.883(11) Å), showing the typical trend of increased bond lengths with increased coordination numbers. A Ge–Ge distance of 3.5127(7) Å rules out a single bond between cations, as observed in various organometallic compounds.[29,30]

Polyhedral distortions in GeP_2N_4 were analyzed calculating the minimal bonding ellipsoids (MBE) using the software PIEFACE, showing regular PN_4-tetrahedra (figure S8).[31] Furthermore, the electrostatic plausibility of the structure model was confirmed by calculating effective charges using the CHARDI and BVS method.[32,33] The
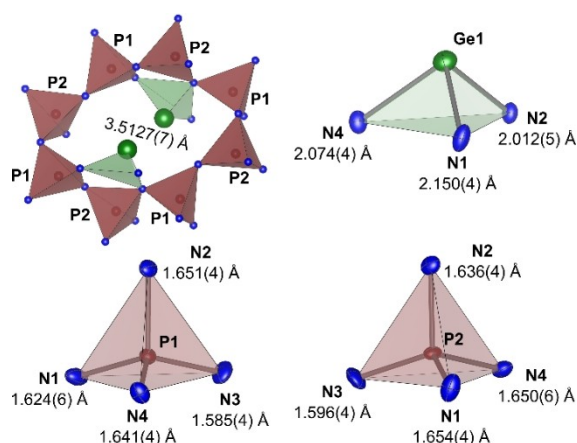
results and more detailed information is provided in the Supporting Information.

Beyond the detailed view on the bonding situation between Ge and N, the electronic structure of GeP_2N_4 was examined by calculating the density of states (DOS) as shown in figure 5. The calculations reveal three distinct regions from −20 eV to −15 eV, from −14 eV to −6 eV and from −6 eV to the fermi edge at 0 eV.

The lowest energy region is almost exclusively dominated by contributions of P and N, equating to strong P–N-bonds, forming the covalent nitridophosphate network. The middle region shows contributions of all elements and is mainly dominated by Ge–N and further contributions of P–N bonds. States close to the fermi edge show a high contribution of Ge, originating from the lone electron pair. Further detailed plots on the density of states can be found in the Supporting Information (figures S9 and S10).

To rule out incomplete condensation and the presence of imide groups, which either may form as contact to air and moisture cannot be completely avoided during synthesis or using NH_4N_3 as a reactant according to equation (2), samples were analyzed by FTIR-spectroscopy (figure S7) and solid-state NMR-spectroscopy (figures 6 and S6).

Figure 3. Coordination polyhedra of P1, P2 and Ge1. The thermal ellipsoids are shown at 90% probability level.

Figure 5. Calculated density of states (DOS) for GeP_2N_4. The total DOS and contributions of individual elements are color-coded.
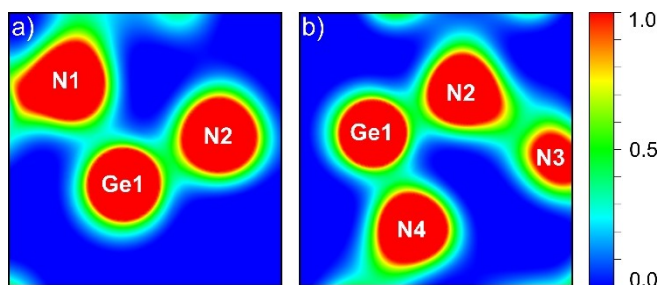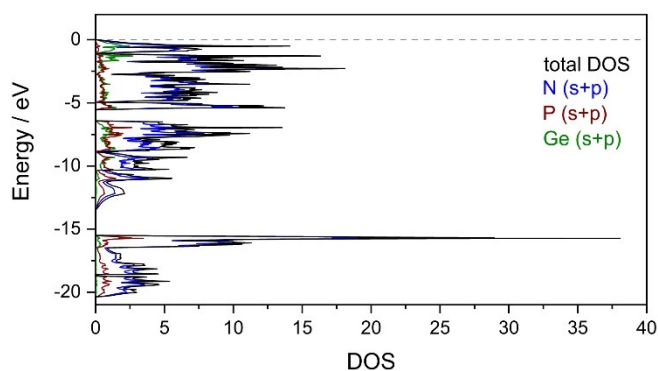
Figure 4. Electron localization plot for visualization of the Ge–N bonding situation. Ge1 forms three bonds to the coordinating atoms N1, N2 and N4. a) Shared electron density between Ge1 and N1/N2. b) Shared electron density between Ge1 and N2/N4. No shared electron density is observed in between Ge1 and N3.
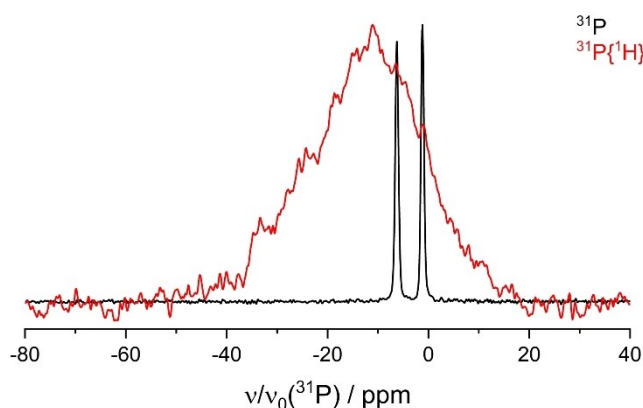
Figure 6. ^{31}P NMR spectrum of GeP_2N_4 (black) showing two signals with intensity ratio 1:1. These signals do not match with the $^{31}P\{^1H\}$ NMR spectrum (red), which indicates the absence of hydrogen in GeP_2N_4.

The ^{31}P-spectrum shows two signals with an integrated intensity ratio of 1:1, which corresponds to two crystallographic P sites with the same multiplicity (4*a*). The chemical shifts ($\delta = -1.20$ ppm, $\delta = -6.27$ ppm) are in the typical range of PN$_4$-tetrahedra next to metal cations, as observed in other MP$_2$N$_4$ (M = Sr, Ba, Mn, Cd) compounds.[18–20] The ^{31}P{^{1}H} cross polarized spectrum contains no signal matching the ^{31}P signals of GeP$_2$N$_4$, indicating the absence of hydrogen in the crystal structure of GeP$_2$N$_4$. Furthermore, the FTIR-spectrum shows no N–H absorption band, which supports all previous results.

As the synthesis of GeP$_2$N$_4$ is extremely sensitive to small changes in temperature, the thermal expansion and stability of GeP$_2$N$_4$ was examined by temperature-dependent powder X-ray diffraction experiments (figure S4). It was found, that GeP$_2$N$_4$ shows an extremely small thermal expansion of the unit cell (average: 10.5 ppm/K) in the range from 25 to 800 °C (figure S5), the critical temperature threshold observed during synthesis. Upon further heating, GeP$_2$N$_4$ decomposes irreversibly into amorphous materials and on cooling no recrystallisation or formation of another compound is observed. Such low thermal expansion, sometimes even negative, is usually observed for zeolites and extremely porous materials and attributed to an internal expansion into the pores of the crystal structure.[34] As GeP$_2$N$_4$ features the same degree of condensation as zeolites as well as large rings containing Ge^{2+}, a similar behavior seems reasonable.

Summarizing, we have synthesized GeP$_2$N$_4$, the first MP$_2$N$_4$ compound with a p-block cation and the first example of a germanium(II) nitridophosphate. The synthesis was carried out under high pressure and high temperature starting from P$_3$N$_5$ and Ge$_3$N$_4$. The structure was determined by single-crystal X-ray diffraction and analyzed for its plausibility by Rietveld-refinement, MBE, CHARDI and BVS calculations. The density of states and bonding situation between Ge and N was theoretically analyzed using DFT calculations and an electron localization function. Further characterization of GeP$_2$N$_4$ was done by means of FTIR- and NMR-spectroscopy and temperature dependent powder X-ray diffraction. As shown here, the formal exchange of alkaline-earth cations with Ge^{2+} is possible, however, leads to a comprehensive structural change due to the stereochemical influence of the lone pair at Ge^{2+}. Using this possibility with other literature-known alkaline-earth nitridophosphates, we expect access to a variety of new structures with intriguing materials properties or even the possibility of targeted structural tuning by mixing germanium with alkaline-earth metals.

Conflict of Interest

The authors declare no conflict of interest.

Data Availability Statement

The data that support the findings of this study are available in the supplementary material of this article.

[1] F. Liebau, *Structural Chemistry of Silicates. Structure, Bonding, and Classification*, Springer, Berlin, **1985**, pp. 1–6. The terms *"vierer ring"* and *"achter ring"* have been defined by Liebau and are derived from the German words "vier" (engl. four) and "acht" (engl. eight), describing rings consisting of the respective amount of tetrahedra.

[2] J. V. Smith, *Acta Crystallogr.* **1953**, *6*, 613.

[3] S. D. Kloss, W. Schnick, *Angew. Chem. Int. Ed.* **2015**, *54*, 11250; *Angew. Chem.* **2015**, *127*, 11402.

[4] L. Eisenburger, P. Strobel, P. J. Schmidt, T. Bräuniger, J. Wright, E. L. Bright, C. Giacobbe, O. Oeckler, W. Schnick, *Angew. Chem. Int. Ed.* **2022**, *61*, e202114902; *Angew. Chem.* **2022**, *134*, e202114902.

[5] J.-M. Léger, J. Haines, L. S. de Oliveira, C. Chateau, A. Le Sauze, R. Marchand, S. Hull, *J. Phys. Chem. Solids* **1999**, *60*, 145.

[6] D. Baumann, S. J. Sedlmaier, W. Schnick, *Angew. Chem. Int. Ed.* **2012**, *51*, 4707; *Angew. Chem.* **2012**, *124*, 4785.

[7] D. Baumann, R. Niklaus, W. Schnick, *Angew. Chem. Int. Ed.* **2015**, *54*, 4388; *Angew. Chem.* **2015**, *127*, 4463.

[8] S. Vogel, D. Baumann, R. Niklaus, E. Bykova, M. Bykov, N. Dubrovinskaia, L. Dubrovinsky, W. Schnick, *Angew. Chem. Int. Ed.* **2018**, *57*, 6691; *Angew. Chem.* **2018**, *130*, 6801.

[9] F. Liebau, *Angew. Chem. Int. Ed.* **1999**, *38*, 1733; *Angew. Chem.* **1999**, *111*, 1845.

[10] A. Stock, H. Grüneberg, *Ber. Dtsch. Chem. Ges.* **1907**, *40*, 2573.

[11] W. Schnick, J. Lücke, *Z. Anorg. Allg. Chem.* **1992**, *610*, 121.

[12] A. Marchuk, F. J. Pucher, F. W. Karau, W. Schnick, *Angew. Chem. Int. Ed.* **2014**, *53*, 2469; *Angew. Chem.* **2014**, *126*, 2501.

[13] W. Schnick, J. Lücke, *Z. Anorg. Allg. Chem.* **1990**, *588*, 19.

[14] W. Schnick, J. Lücke, *Solid State Ionics* **1990**, *38*, 2713.

[15] K. Landskron, S. Schmid, W. Schnick, *Z. Anorg. Allg. Chem.* **2001**, *627*, 2469.

[16] S. Vogel, M. Bykov, E. Bykova, S. Wendl, S. D. Kloß, A. Pakhomova, N. Dubrovinskaia, L. Dubrovinsky, W. Schnick, *Angew. Chem. Int. Ed.* **2020**, *59*, 2730; *Angew. Chem.* **2020**, *132*, 2752.

[17] F. J. Pucher, A. Marchuk, P. J. Schmidt, D. Wiechert, W. Schnick, *Chem. Eur. J.* **2015**, *21*, 6443.

[18] F. W. Karau, W. Schnick, *J. Solid State Chem.* **2005**, *178*, 135.

[19] F. W. Karau, L. Seyfarth, O. Oeckler, J. Senker, K. Landskron, W. Schnick, *Chem. Eur. J.* **2007**, *13*, 6841.

[20] F. J. Pucher, F. W. Karau, J. Schmedt auf der Günne, W. Schnick, *Eur. J. Inorg. Chem.* **2016**, 1497.

[21] A. P. Khomyakov, G. N. Nechelyustov, E. Sokolova, E. Bonaccorsi, S. Merlino, M. Pasero, *Can. Mineral.* **2002**, *40*, 961.

[22] H. Huppertz, *Z. Kristallogr. - Cryst. Mater.* **2004**, *219*, 330.

[23] J. Häusler, L. Eisenburger, O. Oeckler, W. Schnick, *Eur. J. Inorg. Chem.* **2018**, 759.

[24] Deposition number 2210954 contains the supplementary crystallographic data for this paper. These data are provided free of charge by the joint Cambridge Crystallographic Data Centre and Fachinformationszentrum Karlsruhe Access Structures service.

[25] V. A. Blatov, A. P. Shevchenko, D. M. Proserpio, *Cryst. Growth Des.* **2014**, *14*, 3576.

[26] K. Eickmeiner, R. Poschkamp, R. Dronskowski, S. Steinberg, *Eur. J. Inorg. Chem.* **2022**, e202200360.

[27] H. Yamane, F. J. DiSalvo, *J. Alloys Compd.* **1996**, *241*, 69.

[28] M. Everett, A. Jolleys, W. Levason, M. E. Light, D. Pugh, G. Reid, *Dalton Trans.* **2015**, *44*, 20898.

[29] J. Li, C. Schenk, C. Goedecke, G. Frenking, C. Jones, *J. Am. Chem. Soc.* **2011**, *133*, 18622.

[30] S. Nagendran, S. S. Sen, H. W. Roesky, D. Koley, H. Grubmüller, A. Pal, R. Herbst-Irmer, *Organometallics* **2008**, *27*, 5459.

[31] J. Cumby, J. P. Attfield, *Nat. Commun.* **2017**, *8*, 14235.

[32] R. Hoppe, S. Voigt, H. Glaum, J. Kissel, H. P. Müller, K. Bernet, *J. Less-Common Met.* **1989**, *156*, 105.

[33] A. S. Wills, VaList—A bond valence calculation and analysis program, London, **2010**.

[34] P. Tschaufeser, S. C. Parker, *J. Phys. Chem.* **1995**, *99*, 10609.